

# The conditional-mean barrier: From deterministic regression to conditional distribution learning

Junfeng Chen

*Department of Mathematics, The Hong Kong University of Science and Technology, Hong Kong, China*

---

## Abstract

Many problems in computational science and engineering become one-to-many after coarse graining, partial observation, or inverse reconstruction: a resolved state may not determine a unique subgrid forcing, a structural descriptor may not determine a unique effective response, and a low-resolution observation may correspond to many plausible high-resolution fields. In such settings, deterministic surrogates may learn a well-defined mathematical object while still missing the uncertainty that the application requires. This tutorial develops a pedagogically self-contained module centered on the *conditional-mean barrier*: the operating point at which a fitted deterministic predictor has reached the conditional mean  $\mathbb{E}[Y | X]$  and the remaining squared-loss error is the irreducible aleatoric variance. We give two diagnostics for empirically locating this barrier—residual–feature orthogonality and the coefficient of determination against its explained-variance ceiling—and prove a variance-suppression result showing that injecting latent randomness into a squared-loss-trained predictor collapses it back to the conditional mean. Crossing the barrier therefore requires a loss function that scores distributions rather than predictions, and the operative decision is which feature of  $P(Y | X)$  the application requires. We briefly catalog the principal distributional objectives—negative log-likelihood, moment and observable matching, the evidence lower bound, adversarial divergences, and score matching—by the feature of  $P(Y | X)$  each selects, and otherwise refer the reader to the dedicated literature. The emphasis throughout is the boundary itself, together with a finite-data procedure for recognizing it, rather than a survey of the methods beyond it. Reproducible CPU-based demonstrations on a two-branch law and a two-scale Lorenz–96 closure problem show how the diagnostics distinguish deterministic underfitting from residual distributional variability.

*Keywords:* computational science and engineering, regression, conditional mean, residual orthogonality, variance suppression, conditional distribution learning

*2000 MSC:* 37N10, 62J02, 62J20, 68T07, 62-01

---

## 1. Introduction

A great deal of computational science and engineering (CSE) can be cast as the problem of fitting an unknown function from data. Given pairs  $(x_i, y_i)$ , one seeks  $f$  such that  $y \approx f(x)$ . Data-driven discovery of governing equations and closure terms [1, 2, 3], surrogate modeling for computationally expensive equations [4, 5], and regularized inverse reconstruction [6, 7] all often take a deterministic input–output relation as the object to be learned, with least-squares fitting as standard machinery.

This formulation hides a question that is easy to ask once one notices it: what if the input  $x$  does not, in fact, determine the output  $y$ ? Many problems in CSE have exactly this one-to-many structure after coarse graining or partial observation. Two trajectories of a multiscale dynamical system sharing the same coarse state generally need not share the same future coarse evolution, as unresolved variables induce memory and stochastic effects in the reduced dynamics [8, 9]; a two-dimensional slice or low-dimensional descriptor of a heterogeneous composite is compatible with many three-dimensional microstructures and hence with a spread of effective properties [10, 11]; and, as a visually familiar inverse-reconstruction problem, a low-resolution image is the downsampling limit of many distinct high-resolution images [12, 13]. In each case, “fit a function” is not a property of the underlying physical

---

*Email address:* majfchen@ust.hk (Junfeng Chen)

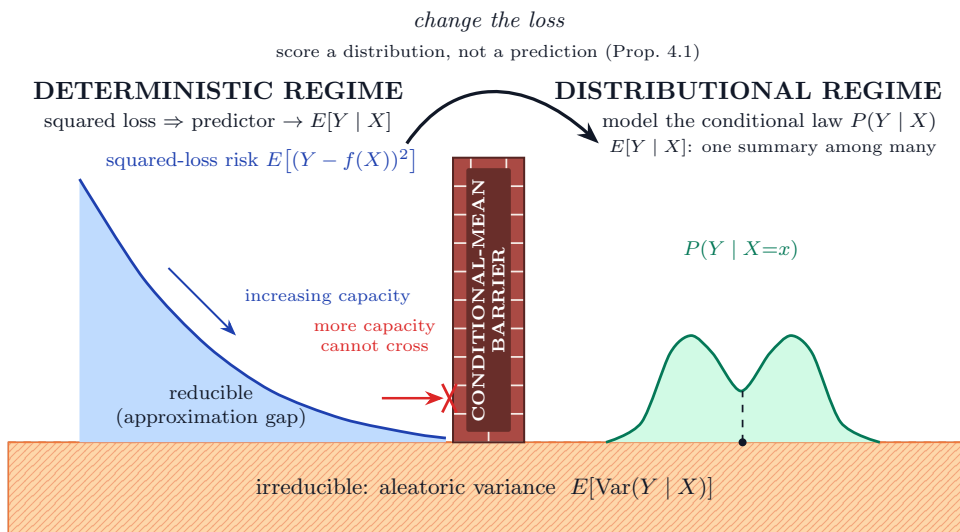


Figure 1. The conditional-mean barrier. In the deterministic regime (left), increasing model capacity drives the squared-loss risk  $E[(Y - f(X))^2]$  down toward the irreducible aleatoric floor  $E[\text{Var}(Y | X)]$  as  $f \rightarrow E[Y | X]$ ; the reducible approximation gap closes, but no squared-loss predictor can pass below the floor, and adding capacity—or latent randomness (proposition 4.1)—does not help. Crossing into the distributional regime (right) requires changing the loss to one that scores a distribution rather than a prediction, after which the object of inference is the conditional law  $P(Y | X)$ , of which the conditional mean is a single summary.

or observational system but a modeling choice, and one that may erase precisely the variability the application cares about.

The mathematical response is to regard deterministic functions as summaries of a richer object: the conditional distribution. Let  $(X, Y)$  be a pair of random variables with joint law  $P_{X,Y}$ . The natural object of inference is the conditional law  $P(Y | X = x)$ , which need not be a point mass. Any deterministic predictor  $\hat{f} : \mathcal{X} \rightarrow \mathcal{Y}$  is a lossy summary of this law, and the form of the summary is determined by the loss function used during training. Under squared loss, the population summary is the conditional mean  $\mathbb{E}[Y | X = x]$  [14, Sec. 2.4][15, Sec. 1.5.5]. Under negative log-likelihood, the population target is the Kullback–Leibler approximation of  $P(Y | X)$  within the chosen parametric family [15, Sec. 1.6] [16, Ch. 2]. Under idealized population and capacity assumptions, adversarial and score-matching objectives target distributional approximations whose induced laws approximate the conditional law [17, 18].

The choice of loss function is therefore the central design decision, but the focus of this tutorial is not the full landscape of distributional losses. It is the boundary between deterministic and distributional learning: the operating point at which a fitted deterministic predictor has converged to the conditional mean and yet the error has not. We call this the *conditional-mean barrier* (fig. 1). The tutorial provides two finite-data diagnostics for locating it—residual–feature orthogonality and the coefficient of determination against its explained-variance ceiling—and a variance-suppression theorem showing that the barrier cannot be crossed by injecting randomness while retaining squared loss: it can be crossed only by changing the loss function. The mathematical ingredients are individually known; the contribution is their integration into a coherent decision procedure, demonstrated in both a controlled synthetic setting and a realistic applied problem.

While pedagogical material on individual statistical and machine-learning methods is now broadly available, the challenge for CSE curricula is often one of integration rather than coverage. The conditional-mean barrier provides such an organizing principle. It starts from least squares and its  $L^2$ -projection interpretation, then identifies the point at which improving a deterministic predictor is no longer the right question. At that point, the modeling target must shift from a point summary to a feature of the conditional law.

The exposition is mathematical rather than algorithmic. It is aimed at advanced undergraduate and beginning graduate students in applied mathematics, computational science, and engineering, as well as researchers familiar with

deterministic regression who want a principled introduction to when and why distributional learning is needed. We assume elementary functional analysis, including Hilbert spaces and  $L^2$  projection, and basic probability through conditional expectation; we do not assume measure-theoretic probability, deep-learning frameworks, or specific machine-learning libraries. The manuscript develops the boundary between deterministic and distributional learning and the finite-data diagnostics for locating it, then signposts the distributional objectives used beyond it.

The remainder of this paper is organized as follows. Section 2 fixes notation and frames the dataset. Section 3 develops the deterministic regime: the finite-dimensional projection view of least squares, the conditional-mean theorem, residual-orthogonality diagnostics, the explained-variance ceiling, and the boundary of squared-loss methods. Section 4 crosses the boundary: it introduces the canonical distributional loss (Kullback–Leibler projection via negative log-likelihood), and proves the variance-suppression theorem that obstructs distribution learning under squared loss. Section 5 briefly catalogs the principal distributional objectives beyond the barrier—negative log-likelihood, moment and observable matching, ELBO, adversarial divergence, and score matching—organized by the feature of  $P(Y | X)$  each selects, and refers the reader to the dedicated literature for the methods themselves. Section 6 gives reproducible demonstrations: a controlled two-branch law, a two-scale Lorenz–96 closure example, and a stochastic closure demonstration showing that a distributional loss substantially mitigates downstream fluctuation suppression caused by the deterministic closure.

## 2. Setup and notation

We work throughout with a pair of random variables  $(X, Y)$  taking values in measurable spaces  $(\mathcal{X}, \mathcal{B}_X)$  and  $(\mathcal{Y}, \mathcal{B}_Y)$ , with joint law  $P_{X,Y}$ . In most examples one may take  $\mathcal{X} \subseteq \mathbb{R}^d$  and  $\mathcal{Y} \subseteq \mathbb{R}^k$ , although the same notation also covers image-valued or function-valued outputs. We write  $P_X$  and  $P_Y$  for the marginals and  $P_{Y|X}$  for the conditional law of  $Y$  given  $X$ . Such a law exists, for example, when the state spaces are standard Borel spaces; this covers the Euclidean settings used in the examples and many separable function-space settings encountered in applications [19, Ch. 5]. Throughout,  $\mathbb{E}$  and  $\text{Var}$  denote expectation and variance under the joint law unless a subscript indicates otherwise.

The joint law  $P_{X,Y}$  is the object we want to learn from, but it is not observed directly. Instead, we observe a finite dataset

$$\mathcal{D}_n = \{(x_i, y_i)\}_{i=1}^n, \quad (x_i, y_i) \stackrel{\text{iid}}{\sim} P_{X,Y}. \quad (1)$$

The i.i.d. assumption is a simplification: data from dynamical systems, inverse solvers, or numerical simulations may be correlated or structured. Those extensions matter in applications, but they are not needed for the population-level questions emphasized here. Under i.i.d. sampling,  $\mathcal{D}_n$  is the finite window through which conditional means, conditional variances, risks, divergences, and sampling laws are estimated.

We will distinguish three data roles. The *training set* is used to fit the model. An independent *diagnostic set* is used to evaluate residual structure, tune simple modeling choices, and assess whether the fitted predictor has reached the conditional-mean barrier. A separate *test set*, when used, is reserved for final held-out evaluation and is not used to choose the model or interpret the residual diagnostics. This distinction is important for the residual-orthogonality diagnostics in Section 3: training residuals may be artificially orthogonal to the features used during fitting, whereas independent diagnostic residuals can reveal structure that the fitted model has not captured. Unless otherwise stated,  $\mathcal{D}_n$  denotes the training set.

A learning procedure is specified by a hypothesis class and a loss function. Its *population risk* is the expected loss under  $P_{X,Y}$ , and its *empirical risk* is the sample average over  $\mathcal{D}_n$ . The Bayes-optimal predictor minimizes the population risk over all admissible candidates; practical methods minimize empirical risk over a restricted class. Approximation error, estimation error, and finite-sample rates are important [20, Ch. 2], but they are not the focus here. The question emphasized in this tutorial is: what population object is selected by a given loss function? Examples that recur throughout the manuscript are the conditional mean under squared loss and the Kullback–Leibler projection under negative log-likelihood.

## 3. Deterministic Regression and the Conditional-Mean Limit

We begin with point prediction: constructing a deterministic function  $\hat{f}: \mathcal{X} \rightarrow \mathcal{Y}$  that returns one value per input. Such a predictor is not the conditional law  $P_{Y|X=x}$  itself, but a point summary of it. Which summary is learned depends

on the loss: squared loss targets a conditional mean, absolute-error loss targets a conditional median, and, in discrete prediction problems, zero-one loss targets a conditional mode. This section focuses on squared loss, the standard starting point for regression and surrogate modeling.

The familiar finite-dimensional example is ordinary least squares in a feature basis [14, Ch. 3]. Given a feature map  $\varphi: \mathcal{X} \rightarrow \mathbb{R}^p$ , consider predictors of the form

$$f_{\beta}(x) = \langle \beta, \varphi(x) \rangle.$$

The empirical least-squares estimator satisfies the normal equations

$$\Phi^{\top}(y - \Phi\hat{\beta}) = 0,$$

where  $\Phi$  has rows  $\varphi(x_i)^{\top}$ . Thus the training residual is orthogonal to the fitted feature space. This is the finite-sample version of a population projection principle: even when the true relationship is not linear in  $\varphi(X)$ , the population least-squares target

$$\beta^{\star} \in \arg \min_{\beta \in \mathbb{R}^p} \mathbb{E}[(Y - \langle \beta, \varphi(X) \rangle)^2]$$

is the best  $L^2$  projection of  $Y$  onto the finite-dimensional span of  $\{\varphi_j(X)\}_{j=1}^p$ .

This finite-dimensional picture contains the two ideas that drive the rest of the section: optimal squared-loss prediction is projection, and residual orthogonality is the certificate of optimality. Replacing the finite feature span by the full space of square-integrable functions of  $X$  leads to the conditional mean.

We now pass from finite-dimensional least-squares projection to its full-function-class limit. The first result identifies the squared-loss-optimal deterministic predictor as  $\mathbb{E}[Y | X]$  for any joint law  $P_{X,Y}$ . We then use residual orthogonality to motivate finite-sample diagnostics, use the coefficient of determination to identify the explained-variance ceiling, and finally characterize the boundary at which deterministic modeling stops capturing the variability present in the joint law.

### 3.1. The conditional mean as $L^2$ -optimal predictor

Releasing the linearity restriction yields the cornerstone of the deterministic theory. For notational simplicity we state the result for scalar  $Y$ ; the vector-valued case follows componentwise under squared Euclidean loss.

**Theorem 3.1** (Optimality of the conditional mean). *Let  $Y$  be square-integrable. Among all measurable  $f: \mathcal{X} \rightarrow \mathbb{R}$  such that  $f(X)$  is square-integrable,*

$$\mathbb{E}[Y | X] = \arg \min_{f \text{ measurable}} \mathbb{E}[(Y - f(X))^2]. \quad (2)$$

*Equivalently,  $Y \mapsto \mathbb{E}[Y | X]$  is the orthogonal projection of  $Y$  onto the closed subspace  $L^2(\sigma(X)) \subseteq L^2(P)$  of square-integrable,  $\sigma(X)$ -measurable random variables.*

*Proof.* Write  $Y = m(X) + W$  with  $m(X) := \mathbb{E}[Y | X]$  and  $W := Y - m(X)$ . By construction  $\mathbb{E}[W | X] = 0$ . For any measurable  $f$ ,

$$\begin{aligned} \mathbb{E}[(Y - f(X))^2] &= \mathbb{E}[(m(X) - f(X) + W)^2] \\ &= \mathbb{E}[(m(X) - f(X))^2] + 2 \mathbb{E}[(m(X) - f(X))W] + \mathbb{E}[W^2]. \end{aligned}$$

The cross term vanishes by the tower property:  $\mathbb{E}[(m(X) - f(X))W] = \mathbb{E}[(m(X) - f(X))\mathbb{E}[W | X]] = 0$ . The first term is minimized at  $f = m$ , and the third equals  $\mathbb{E}[\text{Var}(Y | X)]$ , which is independent of  $f$ .  $\square$

The proof also gives the deterministic squared-loss decomposition

$$\mathbb{E}[(Y - f(X))^2] = \mathbb{E}[(\mathbb{E}[Y | X] - f(X))^2] + \mathbb{E}[\text{Var}(Y | X)]. \quad (3)$$

The first term measures the approximation gap to the conditional mean; the second is the irreducible conditional variability left after the best deterministic prediction has been made.

Two consequences of Theorem 3.1 structure the rest of this section.

First, the conditional mean  $m(\cdot)$  is the Bayes-optimal predictor under squared loss, regardless of  $P_{X,Y}$ . No linearity, no Gaussianity, no additive-noise assumption is required. In the population limit, any sufficiently expressive hypothesis class trained by squared loss is therefore searching for  $m$ . Linear models in rich feature maps, kernel methods [21, 22], and neural networks [23, 24] differ in how they parametrize this search and how they trade approximation against estimation error, not in the population target selected by squared loss.

Second, the irreducible term  $\mathbb{E}[\text{Var}(Y | X)]$  in (3), often called the *aleatoric variance* or *Bayes risk*, is the floor below which no squared-loss method can drop. It is a property of  $P_{X,Y}$ , not of the algorithm. Identifying this floor, and recognizing its appearance in finite-sample diagnostics, is the central practical issue of the deterministic regime.

The theorem says nothing about the conditional mean being a *plausible* output of the underlying joint law. It only says the conditional mean is the best deterministic summary under squared loss. The distinction matters whenever  $P_{Y|X}$  is non-degenerate, and is sharpest in the following example, which we return to throughout this section.

*Example 1* (Two-branch conditional law). Let  $X$  have distribution  $P_X$  on  $\mathcal{X}$ , and let  $a, b : \mathcal{X} \rightarrow \mathbb{R}$  be measurable square-integrable functions with  $a(x) \neq b(x)$  on a set of positive  $P_X$ -measure. Suppose that, for each  $x \in \mathcal{X}$ ,

$$Y | X = x \sim \frac{1}{2} \delta_{a(x)} + \frac{1}{2} \delta_{b(x)}.$$

The conditional mean is

$$m(x) = \mathbb{E}[Y | X = x] = \frac{1}{2}(a(x) + b(x)),$$

which is distinct from both  $a(x)$  and  $b(x)$  wherever the two branches differ. The squared-loss-optimal deterministic predictor is therefore the midpoint of two branches, a value the conditional law  $P_{Y|X=x}$  never realizes at those inputs. The aleatoric variance is

$$\text{Var}(Y | X = x) = \frac{1}{4}(a(x) - b(x))^2,$$

strictly positive wherever the two branches differ.

This simple example is the prototype of the conditional-mean barrier. The squared-loss-optimal predictor lies between the two branches and need not be a plausible realization of  $Y | X = x$ . It already displays the phenomena used throughout this section: irreducible error beyond the conditional mean, an  $R^2$  ceiling below one, and the inadequacy of any single deterministic summary for a non-degenerate conditional law.

### 3.2. Approximation in a complete feature basis

How does one approximate  $m$  in practice? The simplest answer, and the one that exposes the structural similarity between classical and modern methods, is to choose features  $\{\varphi_j\}_{j=1}^p$  and approximate  $m$  by a linear combination  $\sum_j \beta_j \varphi_j$ . Theorem 3.1 guarantees  $m \in L^2(P_X)$ , so the relevant approximation question is whether  $\{\varphi_j\}$  is dense in  $L^2(P_X)$ .

**Definition 3.1** (Complete basis). *A countable family  $\{\varphi_j\}_{j=1}^\infty \subset L^2(P_X)$  is complete in  $L^2(P_X)$  if its linear span is dense in  $L^2(P_X)$ ; equivalently, if every  $g \in L^2(P_X)$  admits a sequence of linear combinations of  $\{\varphi_j\}$  converging to  $g$  in  $L^2(P_X)$ .*

Polynomial bases, Fourier bases, wavelet bases, and—under additional hypotheses on  $P_X$ —Gaussian or sigmoidal radial basis functions are complete [21]. The universal approximation theorems for sigmoidal and ReLU networks [25, 23, 26] extend this picture: with sufficiently many hidden units, neural networks form a dense subset of  $L^2(P_X)$ , and so are, in principle, capable of approximating  $m$  arbitrarily well. The classical and modern theories are continuous; only the parametrization differs.

### 3.3. Diagnostics for empirically approximating the conditional mean

The orthogonality content of Theorem 3.1—that  $Y - m(X)$  is orthogonal to every  $g \in L^2(\sigma(X))$ —gives a population characterization of the conditional mean and motivates a practical diagnostic for  $\hat{f}_n \approx m$ :  $f = m$   $P_X$ -almost surely if and only if

$$\mathbb{E}[(Y - f(X))g(X)] = 0 \quad \text{for every } g \in L^2(\sigma(X)). \quad (4)$$

If  $\{\psi_k\}_{k=1}^\infty \subset L^2(P_X)$  is complete in the sense of Definition 3.1, (4) need only be verified with  $g$  ranging over  $\{\psi_k\}_{k=1}^\infty$ . The forward direction is the cross-term calculation already used in the proof of Theorem 3.1; the reverse direction follows by testing with  $g = m - f$ , and the complete-basis version follows by density in  $L^2(P_X)$ .

Equation (4) and the size of the residual answer two logically independent questions, and it is their pairing—not either one alone—that constitutes the diagnosis. The orthogonality condition is a question about the *model*: has the fit extracted all the deterministic signal that  $X$  carries about  $Y$ , or does reducible structure remain? It is direction-resolved—a nonzero inner product in (4) not only flags inadequacy but names the direction  $\psi$  along which the residual still varies, and hence the feature one should add. The residual mean-square  $\mathbb{E}[(Y - \hat{f}_n(X))^2]$  is a question about the *task*: granting that no more signal can be extracted, is the variance that remains small enough for the application? It is aggregate—a single scalar that quantifies how much error is left but says nothing about where. A model can be optimal for the first question and inadequate for the second (Regime III below), or the reverse. Keeping the two axes separate is what makes the diagnosis a decision rule rather than a goodness-of-fit verdict.

In finite samples each orthogonality condition is estimated by the empirical inner product

$$T_n(\psi) := \frac{1}{\sqrt{n}} \sum_{i=1}^n \hat{r}_i \psi(x_i), \quad \hat{r}_i := y_i - \hat{f}_n(x_i), \quad (5)$$

which under the ideal null  $\hat{f}_n = m$  and standard moment conditions is asymptotically Gaussian with variance  $\mathbb{E}[\text{Var}(Y | X)\psi(X)^2]$  [27]. Dividing by an estimate of that standard deviation gives the *t-statistic*  $t_n(\psi) = T_n(\psi)/\hat{\sigma}(\psi)$ , with  $\hat{\sigma}(\psi)^2 = n^{-1} \sum_i \hat{r}_i^2 \psi(x_i)^2$ ; under the null  $t_n(\psi)$  is approximately standard normal, and we call a probe *significant* when  $|t_n(\psi)|$  exceeds a certain critical value—the usual evidence that the residual carries a real trend along  $\psi$ .

A significant probe certifies that a residual trend is real, but the threshold for “real” is not fixed: because  $t_n(\psi)$  grows like  $\sqrt{n}$  times the underlying residual–probe correlation, a larger diagnostic set resolves ever-smaller trends. This is the test behaving exactly as it should, but it makes significance a moving target for a *stopping* rule—the same model can be judged adequate on a small diagnostic set and inadequate on a larger one, with no change in the model or the data-generating law. A decision rule must instead compare against a target fixed by the task, not by  $n$ . We therefore pair the test with an *effect size*. For a probe standardized to zero mean and unit variance on the diagnostic set,

$$e_n(\psi) := \frac{T_n(\psi)^2}{n \hat{\sigma}_r^2}, \quad \hat{\sigma}_r^2 := \frac{1}{n} \sum_{i=1}^n \hat{r}_i^2, \quad (6)$$

is the squared residual–probe correlation, i.e. the fraction of residual variance that a linear correction along  $\psi$  would remove; unlike significance, it measures how much a trend matters rather than merely whether it exists. Finally, the residual mean-square itself estimates the irreducible floor: by the squared-loss decomposition (3), the population residual mean-square is the floor  $\mathbb{E}[\text{Var}(Y | X)]$  plus the non-negative approximation gap  $\mathbb{E}[(m(X) - \hat{f}_n(X))^2]$ , so  $\hat{\sigma}_r^2$  estimates  $\mathbb{E}[\text{Var}(Y | X)]$  *from above*, with the over-estimate equal to the approximation gap that the orthogonality diagnostic is designed to detect. As the diagnostic drives that gap toward zero,  $\hat{\sigma}_r^2 \rightarrow \mathbb{E}[\text{Var}(Y | X)]$ : the same probe family that certifies  $\hat{f}_n \approx m$  also turns the observed residual variance into an estimate of the floor. This is what lets the procedure locate the floor in settings—such as the Lorenz–96 closure of Section 6.2—where it is not available in closed form.

### Procedure 1 (Residual–feature diagnostic).

1. *Probe schedule.* Fix a nested sequence of probe families  $\Psi_1 \subset \Psi_2 \subset \dots \subset L^2(P_X)$  that enriches the fitting basis toward completeness—e.g. monomials and alternative bases. The Bonferroni correction in the next step guards against flagging a probe when no real trend is present; it does nothing to guard against the opposite failure, in which a genuinely inadequate model passes simply because the chosen probes happen to miss the directions where residual structure lives. Enriching the family is the only protection against that second failure—and, since the conclusion of interest is “stop improving,” it is the more dangerous one.
2. *Out-of-basis evaluation on independent data.* On a diagnostic set disjoint from the training data, compute  $t_n(\psi)$  and  $e_n(\psi)$  for every  $\psi$  in the current family whose total degree exceeds that of the fitted basis. Apply a Bonferroni (or comparable) correction within each family, testing at per-probe level  $\alpha/|\Psi_j|$  so the family-wise false-positive rate is held at  $\alpha = 0.05$ .

Table 1. The diagnostic decision rule. Rows: does the orthogonality test detect reducible out-of-basis structure? Columns: is the residual mean-square  $\hat{\sigma}_r^2$  within the downstream task’s tolerance? Each cell gives the regime and the action it licenses.

	<b>Residual within tolerance</b> ( $\hat{\sigma}_r^2 \leq \text{task tolerance}$ )	<b>Residual exceeds tolerance</b> ( $\hat{\sigma}_r^2 > \text{task tolerance}$ )
<b>Structure detected</b> (some $\psi$ : $t_n$ significant, $e_n > \varepsilon$ )	<i>Regime I' (refine)</i> . A reducible trend remains but the error is already acceptable. Extracting it is optional; the barrier is not the binding constraint.	<i>Regime I (underfitting)</i> . Reducible structure and intolerable error. Act on the flagged directions: enlarge the class, change the basis, improve optimization, or collect more data.
<b>No structure detected</b> (all $\psi$ : $e_n \leq \varepsilon$ )	<i>Regime II (adequate)</i> . $\hat{f}_n \approx m$ and the floor is acceptable. Stop; deterministic squared-loss modeling suffices.	<i>Regime III (the barrier)</i> . $\hat{f}_n \approx m$ yet the residual is intolerable: the error is dominated by $\mathbb{E}[\text{Var}(Y   X)]$ . Enlarging the deterministic class cannot help—change the loss, not the model.

3. *Stop rule*. Across the schedule, declare the barrier reached when no out-of-basis probe is both significant *and* practically large—operationally, when  $\max_{\psi} e_n(\psi) \leq \varepsilon$  for a task-set tolerance  $\varepsilon$  fixed independently of  $n$ —and when enriching the family further no longer reduces  $\hat{\sigma}_r^2$  beyond sampling noise. Significance plays only a supporting role: it flags which directions, if any, still carry real structure worth removing, while  $\varepsilon$  decides whether that structure is large enough to matter. These conditions license reading  $\hat{\sigma}_r^2$  as the estimated aleatoric floor  $\mathbb{E}[\text{Var}(Y | X)]$ .

Two features distinguish this from a routine specification test. First, the conclusion that most often matters here—“stop enlarging the deterministic model”—is reached by *failing* to find structure, not by finding it. The dangerous mistake is therefore the one identified in Step 1: passing an inadequate model because the probes happened to miss its structure. Step 3 guards against it by phrasing the barrier as an *equivalence*-style statement (no out-of-basis direction removes more than  $\varepsilon$  of the residual variance) that must remain *stable* as the probe family is enriched, rather than as a single passing test. Second, the diagnostic must use independent data and out-of-basis probes. For OLS in the basis  $\{\varphi_j\}_{j=1}^p$  the normal equations force the training residual to be orthogonal to the fitted features, and for other empirical risk minimizers the in-basis moments are near zero at convergence; in-basis checks therefore carry almost no information about whether  $\hat{f}_n \approx m$ . The substantive test exercises directions in  $L^2(P_X)$  that the fit was not constrained to capture. The common practice of partitioning  $\mathcal{X}$  into regions  $\{A_\ell\}$  and inspecting within-stratum mean residuals is the special case  $\psi_\ell = \mathbf{1}_{A_\ell}$ , and is subsumed by (4).

*A two-axis taxonomy*. The two questions are binary—reducible structure either is or is not detected, and the residual either is or is not within the task’s tolerance—so together they partition the possibilities into four cases, shown in Table 1. The fourth, easily overlooked, is the one in which a small but real nonlinearity coexists with error that is already acceptable: detectable, yet not worth removing.

The high-error column carries the design message. Regime I localizes *and* quantifies a deficiency the practitioner can remove; Regime III certifies that no deterministic remedy exists and that the remaining variance, if the task needs it, must be modeled distributionally. The within-tolerance column gives the cautions: Regime II warns against chasing distributional machinery the application does not require, and Regime I' warns that statistical significance alone—absent the effect size (6)—can recommend effort with negligible payoff. Regime III is the operating point for the remainder of the paper: that of Example 1, of closure problems with genuine subgrid randomness, and of one-to-many inverse problems.

### 3.4. The explained-variance ceiling and the boundary of deterministic modeling

The diagnostic of Section 3.3 already produces a magnitude summary—the residual mean-square  $\hat{\sigma}_r^2$ , which at the barrier estimates the aleatoric floor  $\mathbb{E}[\text{Var}(Y | X)]$ . Expressing that floor as a fraction of the total variance  $\text{Var}(Y)$  turns it into a scale-free ceiling and yields the familiar *coefficient of determination*,

$$R^2(f) := 1 - \frac{\mathbb{E}[(Y - f(X))^2]}{\text{Var}(Y)}, \quad (7)$$

which aggregates the feature-by-feature and stratum-by-stratum agreement of Section 3.3 into a single scalar. Despite its ubiquity,  $R^2$  is most useful when read against the irreducible ceiling we now identify. Substituting the deterministic squared-loss decomposition (3) into (7) gives

$$R^2(f) = 1 - \frac{\mathbb{E}[(m(X) - f(X))^2] + \mathbb{E}[\text{Var}(Y | X)]}{\text{Var}(Y)}, \quad (8)$$

decomposing the gap from one into an *approximation gap*  $\mathbb{E}[(m(X) - f(X))^2]$  and the *irreducible aleatoric variance*  $\mathbb{E}[\text{Var}(Y | X)]$ . Setting  $f = m$  gives the ceiling on  $R^2$ :

$$R^2(m) = 1 - \frac{\mathbb{E}[\text{Var}(Y | X)]}{\text{Var}(Y)} = \frac{\text{Var}(\mathbb{E}[Y | X])}{\text{Var}(Y)} \in [0, 1], \quad (9)$$

the population *correlation ratio*  $\text{Var}(\mathbb{E}[Y | X]) / \text{Var}(Y)$ , whose identity with  $1 - \mathbb{E}[\text{Var}(Y | X)] / \text{Var}(Y)$  is the law of total variance [28, Ch. 3].

The practical message of (9) is fundamental and, in our experience, the single most under-appreciated point in applied regression. At this ceiling, an  $R^2$  value of, say, 0.7 does *not* indicate a poor deterministic model. It indicates that, under  $P_{X,Y}$ , the conditional mean  $\mathbb{E}[Y | X]$  explains seventy percent of the variance in  $Y$ , while the remaining thirty percent is the variance of  $Y$  given  $X$ . No method targeting  $\mathbb{E}[Y | X]$  can recover this remaining variance, because the remaining variance is, by definition, not in the conditional mean. The practitioner facing such an  $R^2$  ceiling has reached the boundary of the deterministic paradigm and must decide whether to accept the floor or to change the question.

That boundary is sharp. Because capacity—polynomial degree, kernel bandwidth, network width and depth—acts only on the approximation gap in (8) and never on the aleatoric term, the ceiling (9) is the best any squared-loss method can reach. When  $P_{Y|X=x}$  is a point mass  $P_X$ -almost surely the aleatoric term vanishes,  $R^2(m) = 1$ , and deterministic modeling is fully adequate; otherwise  $R^2(m) < 1$ , and the shortfall is exactly the information about the conditional law that squared loss cannot see.

The motivating examples of Section 1 are precisely the settings in which this shortfall becomes binding: in closure modeling, super-resolution, and microstructure–property prediction, the variability of  $Y$  given  $X$  may encode what the downstream user requires—unresolved forcing fluctuations, plausible high-frequency detail, or certification-relevant spread in effective properties. Replacing the mean by another deterministic summary—a median, a quantile, or a mode where it exists—changes the point summary being learned but not the underlying nonuniqueness; a single point cannot faithfully represent a broad or multimodal conditional law. The next section accordingly takes the full conditional law as the object to recover, with deterministic summaries available as post-processing.

#### 4. When the mean is not enough: probabilistic regression

The deterministic theory of Section 3 terminates at the conditional mean. To go further—to learn  $P_{Y|X}$  itself rather than its first moment—we must adopt a different goal and a different loss.

*Distributional modeling.* Construct a family  $\{\hat{q}(\cdot | x)\}_{x \in \mathcal{X}}$  of probability measures on  $\mathcal{Y}$  approximating  $P_{Y|X=x}$ . The output is no longer a single value but a distribution per input, typically described through a density, moments, quantiles, or samples.

The appropriate loss is no longer pointwise in the same sense as squared error. A distributional predictor should be judged by how well its law matches the conditional law of the data. The canonical likelihood-based choice is the negative log-density  $-\log q(y | x)$ . This section explains why negative log-likelihood corresponds, at the population level, to a Kullback–Leibler approximation of the true conditional density by the chosen model family. It then culminates in the variance-suppression result showing why squared loss cannot learn a conditional distribution by merely injecting latent randomness.

#### 4.1. Parametric conditional models and maximum likelihood

Fix a parametric family  $\{q_\theta(\cdot | x) : \theta \in \Theta, x \in X\}$  of conditional densities on  $\mathcal{Y}$ . The classical Gaussian regression model with input-dependent mean and variance,

$$q_\theta(y | x) = \mathcal{N}(y; \mu_\theta(x), \Sigma_\theta(x)), \quad (10)$$

is the prototype, with  $(\mu_\theta, \Sigma_\theta)$  a pair of functions parametrized, for example, by neural networks [29, 15].

The likelihood-based analogue of squared-loss risk is the population negative log-likelihood

$$\mathcal{L}(\theta) := \mathbb{E}_{(X,Y) \sim P_{X,Y}}[-\log q_\theta(Y | X)]. \quad (11)$$

This objective rewards a model for assigning high density to the observed output. The population object selected by this loss is most clearly described using the Kullback–Leibler divergence.

**Definition 4.1** (Kullback–Leibler divergence). *Let  $p$  and  $q$  be probability density functions on  $\mathcal{Y}$ . The Kullback–Leibler divergence from  $p$  to  $q$  is*

$$D_{\text{KL}}(p \| q) := \int_{\mathcal{Y}} p(y) \log \frac{p(y)}{q(y)} dy, \quad (12)$$

with the convention  $D_{\text{KL}}(p \| q) = +\infty$  if  $q(y) = 0$  on a set where  $p(y) > 0$ . The divergence is non-negative and vanishes if and only if  $p = q$  almost everywhere [16, Ch. 2]; it is generally asymmetric and so is not a metric.

A more general measure-theoretic version replaces the density ratio  $p/q$  by the Radon–Nikodym derivative [30, Ch. 6.4], but the density form above is sufficient for the present exposition.

To see why negative log-likelihood induces a KL approximation, fix  $x$  and let  $p_{Y|X}(\cdot | x)$  denote the true conditional density. Then

$$\mathbb{E}_{Y \sim P_{Y|X=x}}[-\log q_\theta(Y | x)] \quad (13)$$

$$= - \int_{\mathcal{Y}} p_{Y|X}(y | x) \log q_\theta(y | x) dy \quad (14)$$

$$= \int_{\mathcal{Y}} p_{Y|X}(y | x) \log \frac{p_{Y|X}(y | x)}{q_\theta(y | x)} dy - \int_{\mathcal{Y}} p_{Y|X}(y | x) \log p_{Y|X}(y | x) dy \quad (15)$$

$$= D_{\text{KL}}(p_{Y|X}(\cdot | x) \| q_\theta(\cdot | x)) + H(p_{Y|X}(\cdot | x)), \quad (16)$$

where

$$H(p_{Y|X}(\cdot | x)) := - \int_{\mathcal{Y}} p_{Y|X}(y | x) \log p_{Y|X}(y | x) dy$$

is independent of  $\theta$ . Taking expectations over  $X$  shows that minimizing the population negative log-likelihood is equivalent to minimizing the expected KL divergence

$$\theta^* \in \arg \min_{\theta} \mathbb{E}_X[D_{\text{KL}}(p_{Y|X}(\cdot | X) \| q_\theta(\cdot | X))]. \quad (17)$$

The empirical maximum-likelihood estimator is the sample approximation of this population problem:

$$\hat{\theta}_n \in \arg \min_{\theta \in \Theta} -\frac{1}{n} \sum_{i=1}^n \log q_\theta(y_i | x_i). \quad (18)$$

Maximum-likelihood training therefore chooses, within the prescribed family, the conditional densities closest in expected KL divergence to the truth. Before turning to the distributional losses in Section 5, we first isolate the obstruction that prevents squared loss itself from learning a conditional distribution, even when latent randomness is built into the predictor.

#### 4.2. Why squared loss cannot learn a conditional distribution

We now isolate the obstruction that prevents squared loss from learning a conditional distribution. Suppose that, instead of returning a deterministic point prediction, the model receives an additional latent variable

$$Z \sim p_Z,$$

independent of  $(X, Y)$ , and returns

$$g_\theta(X, Z). \quad (19)$$

For each fixed  $x$ , the randomness in  $Z$  induces a model distribution for the output. This is the same formal device used by many conditional generative models [17, 31], although here we ask a more elementary question: what happens if such a stochastic predictor is still trained by paired squared loss?

Consider the objective

$$\mathcal{L}(\theta) := \mathbb{E}_{(X,Y) \sim P_{X,Y}} \mathbb{E}_{Z \sim p_Z} [(Y - g_\theta(X, Z))^2]. \quad (20)$$

One might hope that the stochasticity in  $Z$ , combined with the flexibility of  $g_\theta$ , would induce the model to spread its mass to match  $P_{Y|X}$ . It does not. The result is elementary and worth stating in isolation.

**Proposition 4.1** (Variance suppression under squared loss). *Let  $g_\theta: \mathcal{X} \times \mathcal{Z} \rightarrow \mathbb{R}$  be measurable and square-integrable for each  $\theta$ , and let  $\mathcal{L}$  be as in (20). Then*

$$\mathcal{L}(\theta) = \mathbb{E}_X[\text{Var}(Y | X)] + \mathbb{E}_X[(\mathbb{E}[Y | X] - \mathbb{E}_Z[g_\theta(X, Z)])^2] + \mathbb{E}_X[\text{Var}_Z(g_\theta(X, Z))]. \quad (21)$$

*In particular, the minimizer over  $\theta$ , taken over a sufficiently expressive family, satisfies  $\mathbb{E}_Z[g_\theta(X, Z)] = \mathbb{E}[Y | X]$  almost surely and  $\text{Var}_Z(g_\theta(X, Z)) = 0$  almost surely. That is,  $g_\theta$  collapses to a deterministic function of  $X$  equal to the conditional mean.*

*Proof.* Expand the squared loss as  $\mathbb{E}[(Y - \mathbb{E}[Y | X] + \mathbb{E}[Y | X] - g_\theta(X, Z))^2]$  and use the tower property to vanish the cross term, yielding

$$\mathcal{L}(\theta) = \mathbb{E}[\text{Var}(Y | X)] + \mathbb{E}[(\mathbb{E}[Y | X] - g_\theta(X, Z))^2].$$

Now apply the same decomposition to the second term with respect to  $Z$ :

$$\mathbb{E}[(\mathbb{E}[Y | X] - g_\theta(X, Z))^2] = \mathbb{E}[(\mathbb{E}[Y | X] - \mathbb{E}_Z g_\theta(X, Z))^2] + \mathbb{E}[\text{Var}_Z g_\theta(X, Z)].$$

Both  $\theta$ -dependent terms in (21) are non-negative, so the minimizer drives each to zero.  $\square$

*Remark 4.1.* Modern uncertainty-quantification practice distinguishes *aleatoric* uncertainty, intrinsic to the joint law  $P_{X,Y}$ , from *epistemic* uncertainty, reflecting finite-data ignorance about a chosen model [32]. In this language, the irreducible term  $\mathbb{E}[\text{Var}(Y | X)]$  in the squared-loss decomposition (3) is aleatoric—a property of  $P_{X,Y}$  that no choice of  $f$  can reduce. The remaining approximation gap  $\mathbb{E}[(m(X) - f(X))^2]$  is the model-side error customarily identified with the epistemic component, since it depends on the hypothesis class, the training data, and the optimizer. Proposition 4.1 then asserts that squared loss obstructs the aleatoric component specifically: posterior averaging over  $\theta$ , ensembling, and similar Bayesian or quasi-Bayesian devices can shrink the epistemic component but cannot manufacture the aleatoric one. For that, the loss must change.

The content of Proposition 4.1 is that squared loss *cannot be salvaged* by injecting stochasticity into the model. The loss treats variance in  $g_\theta(X, Z)$  as cost, regardless of whether that variance matches  $\text{Var}(Y | X)$ . The minimizer is the deterministic predictor of the conditional mean, exactly as in Section 3. To learn the conditional variance, let alone the full conditional law, the loss must penalize distributional mismatch, not pointwise error.

Table 2. Learning objectives and their population targets. The first row is the deterministic squared-loss baseline; the remaining rows use objectives that capture information beyond the conditional mean.

Loss / objective	Population target	Representative models
Squared loss	Conditional mean $\mathbb{E}[Y   X]$	Linear regression; kernel and neural regressors
NLL on parametric family	Expected KL approximation of $P_{Y X}$ within the family	Heteroscedastic Gaussian regression; normalizing flows
Moment / observable matching	Selected conditional moments or task-relevant observables	Moment-matched stochastic closures; calibrated simulators
ELBO	Variational lower bound on conditional log-likelihood	Variational autoencoders
Adversarial divergence	Distributional match in a learned metric or discriminator class	Generative adversarial networks
Score matching	Score field $\nabla_y \log p_r(y   x)$ along a noising path	Diffusion / score-based models

## 5. Beyond the barrier: choosing a distributional loss

Proposition 4.1 establishes that crossing the conditional-mean barrier requires a loss function that scores distributions, not predictions. Many such losses exist, and the unifying observation—the one this module aims to leave the reader with—is that each commits to a different feature of  $P_{Y|X}$ . The first modeling decision is therefore not which generative architecture to adopt, but which feature of the conditional law the downstream task requires. If the task depends only on first-moment prediction, the conditional mean already suffices and the barrier is irrelevant. If calibrated variances, tail probabilities, fluxes, spectra, or other observables are required, an objective that scores those quantities is appropriate; if the task needs plausible samples from a high-dimensional conditional law, an implicit or score-based sampler becomes natural. Table 2 records the principal objectives, the population target each selects, and representative model classes. What matters here is the column of population targets, not the algorithms, whose derivations and implementation we leave to the dedicated literature.

Two entries connect directly to the preceding sections. Negative log-likelihood on a parametric family  $\{q_\theta(\cdot | x)\}_{\theta \in \Theta}$  is the empirical counterpart of the expected-KL problem (17) derived in Section 4, via the cross-entropy decomposition (16), and is the most direct repair of the variance-suppression obstruction: heteroscedastic Gaussian regression [29, 15, 33] and conditional normalizing flows [34, 35, 36] are standard instances, and the learned-scale closure of Section 6.3 is a minimal example. The remaining objectives—moment and observable matching [27, 37, 38], the evidence lower bound of variational autoencoders [31, 39, 40], adversarial divergences [17, 41, 42], and the score-matching  $L^2$  objective underlying diffusion models [18, 43, 44, 45]—share the property that, unlike paired squared loss, they score distributions and therefore do not force injected randomness to collapse (Proposition 4.1). They differ in what they assume and what they return: a tractable density, a finite collection of observables, or a sampler with no explicit density. We do not develop them here; the purpose of this module is the boundary and its diagnosis, with the far side signposted rather than surveyed.

## 6. Demonstration examples

The numerical demonstrations are intended as teaching examples rather than performance benchmarks. All scripts run on CPU by default, with fixed random seeds and single-threaded execution to reduce backend-dependent variation. We use modest sample sizes, and adopt Legendre polynomials as the backbone regressor.

### 6.1. A controlled two-branch law

We first return to the two-branch construction of Example 1, now with all population quantities known in closed form. Let

$$X \sim \text{Unif}[-1, 1], \quad B \in \{-1, 1\}, \quad \mathbb{P}(B = 1) = \mathbb{P}(B = -1) = \frac{1}{2},$$

and define

$$Y = m(X) + B a(X), \quad m(x) = \sin(2\pi x), \quad a(x) = 0.5 + 0.3 \cos(2\pi x). \quad (22)$$

Then

$$\mathbb{E}[Y | X = x] = m(x), \quad \text{Var}(Y | X = x) = a(x)^2.$$

For this law,

$$\text{Var}(m(X)) = \frac{1}{2}, \quad \mathbb{E}[\text{Var}(Y | X)] = \mathbb{E}[a(X)^2] = 0.295,$$

and therefore

$$\text{Var}(Y) = 0.795, \quad R^2(m) = \frac{\text{Var}(m(X))}{\text{Var}(Y)} = \frac{0.5}{0.795} \approx 0.629. \quad (23)$$

Thus, even a perfect squared-loss predictor cannot attain  $R^2 = 1$ : roughly 37% of the variance in  $Y$  is irreducible conditional variability.

We generated 800 training samples, 2,000 independent diagnostic samples, and 5,000 independent test samples from (22). The diagnostic set is chosen larger than the training set so that residual moments are estimated with visibly smaller sampling noise, while the test set is used only to estimate the  $R^2$  curve. Deterministic predictors were fitted by least squares in the Legendre basis

$$\hat{f}_p(x) = \sum_{j=0}^p \hat{\beta}_j P_j(x),$$

where  $P_j$  is the  $j$ -th Legendre polynomial on  $[-1, 1]$ . We use  $p = 2$  as a deliberately underfit model and  $p = 9$  as a high-capacity representative. The whole degree path  $p = 0, \dots, 30$  is also computed to visualize the explained-variance ceiling.

Figure 2(a) shows the sampled two-branch law, the true conditional mean  $m$ , and the two least-squares fits. The degree-2 model misses the oscillatory conditional mean and leaves substantial deterministic structure in the residual. By contrast, the degree-9 model tracks  $m$  closely. Notice that the fitted curve lies between the two branches: it is the squared-loss-optimal deterministic summary, not a typical realization of  $Y | X = x$ .

Figure 2(b) plots the test  $R^2$  as the polynomial degree increases. The curve rises quickly and then saturates near the theoretical ceiling (23). For  $p = 9$ , the test error is approximately

$$\text{MSE}_{\text{test}}(\hat{f}_9) \approx 0.302, \quad R_{\text{test}}^2(\hat{f}_9) \approx 0.620,$$

close to the Bayes risk 0.295 and the ceiling 0.629. Increasing capacity beyond this point does not move the deterministic predictor toward  $R^2 = 1$ , because the remaining error is dominated by  $\mathbb{E}[\text{Var}(Y | X)]$ .

The residual–feature diagnostic gives the complementary view, pairing the two statistics of Procedure 1. On the  $n = 2000$  diagnostic samples we evaluate the significance  $t_n(\psi)$  and the effect size  $e_n(\psi)$  of Section 3.3 (the latter is (6)), taking  $\psi$  to be the orthonormalized Legendre probes  $\sqrt{2k+1} P_k$ ; the factor  $\sqrt{2k+1}$  gives unit variance under  $X \sim \text{Unif}[-1, 1]$ , so  $e_n$  reads directly as the fraction of residual variance a correction along  $P_k$  would remove. We fix the task tolerance at  $\varepsilon = 0.01$ .

Figure 3 reports both statistics for the out-of-basis probes. For the degree-2 fit the residual carries structure that is both significant and practically large: the worst direction  $P_5$  reaches  $|t_n| \approx 34$  and  $e_n \approx 0.43$ , so a single Legendre correction would remove about 43% of the residual variance, far above  $\varepsilon$ . Together with its large prediction error this places the degree-2 model in Regime I (deterministic underfitting, Table 1): the flagged directions are exactly the missing oscillatory structure, and enlarging the basis is the right remedy. For the degree-9 fit no out-of-basis probe is either significant or large—maximum  $|t_n| \approx 1.3$  and maximum  $e_n \approx 1 \times 10^{-3}$ , well below  $\varepsilon$ —so the orthogonality diagnostic is satisfied. Its residual mean-square is not small, however: on the diagnostic set  $\hat{\sigma}_r^2 \approx 0.296$ , essentially the Bayes floor  $\mathbb{E}[\text{Var}(Y | X)] = 0.295$ . The degree-9 fit therefore sits at the conditional-mean barrier (Regime III): it has reached  $m$ , the diagnostic has located the aleatoric floor from data, and the remaining error is irreducible by any squared-loss method. The same prediction-error level thus carries two different verdicts—learnable deterministic structure for  $p = 2$ , the barrier for  $p = 9$ —and it is the pairing of significance with effect size, not either alone, that separates them.

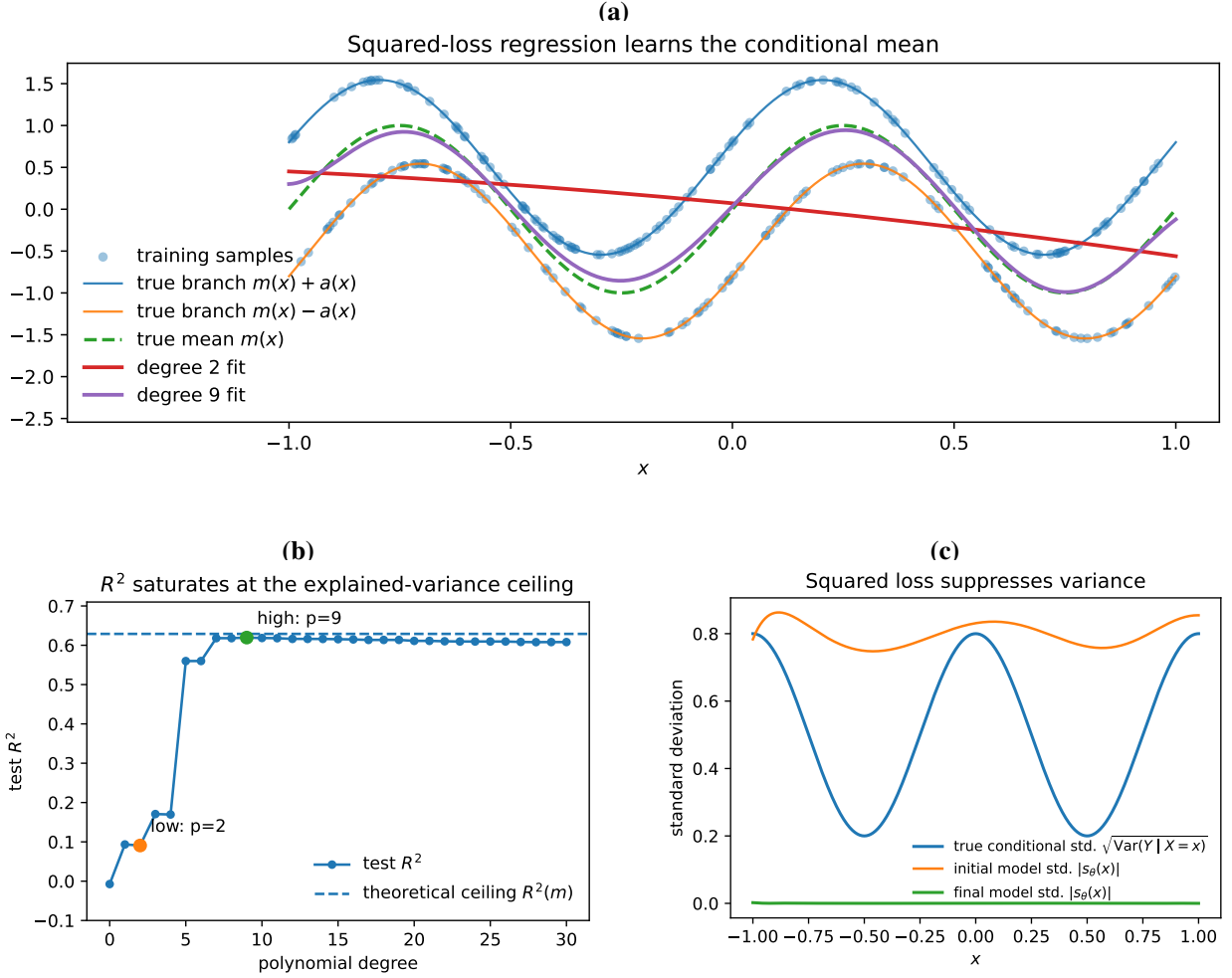


Figure 2. A controlled two-branch experiment. (a) Samples from (22), the two branches  $m(x) \pm a(x)$ , the true conditional mean  $m(x)$ , and two deterministic least-squares fits. (b) Test  $R^2$  versus polynomial degree, saturating at the explained-variance ceiling (23). (c) Variance suppression for a stochastic predictor  $g_\theta(x, Z) = \mu_\theta(x) + s_\theta(x)Z$  trained by squared loss.

Finally, we illustrate Proposition 4.1. We train a stochastic predictor of the form

$$g_\theta(x, Z) = \mu_\theta(x) + s_\theta(x)Z, \quad Z \sim \mathcal{N}(0, 1),$$

where both  $\mu_\theta$  and  $s_\theta$  are represented in the same Legendre basis. For fixed  $x$ , this model has conditional variance

$$\text{Var}_Z(g_\theta(x, Z)) = s_\theta(x)^2.$$

It might therefore appear capable of learning the nonzero conditional variance  $a(x)^2$ . However, for this model the decomposition of Proposition 4.1 reads  $\mathbb{E}_{X,Y,Z}[(Y - g_\theta(X, Z))^2] = \mathbb{E}_{X,Y}[(Y - \mu_\theta(X))^2] + \mathbb{E}_X[s_\theta(X)^2]$ , so the model variance is penalized directly. Figure 2(c) shows the consequence: although the true conditional standard deviation  $a(x)$  is nonzero and the model is initialized with a nonzero stochastic scale, the learned scale  $s_\theta(x)$  collapses to essentially zero. Numerically,  $\mathbb{E}_X[s_\theta(X)^2]$  decreases from approximately  $6.4 \times 10^{-1}$  to  $1.0 \times 10^{-7}$ . The learned stochastic model therefore reduces to the deterministic conditional-mean predictor. This is the variance-suppression theorem made visible in the simplest possible setting.

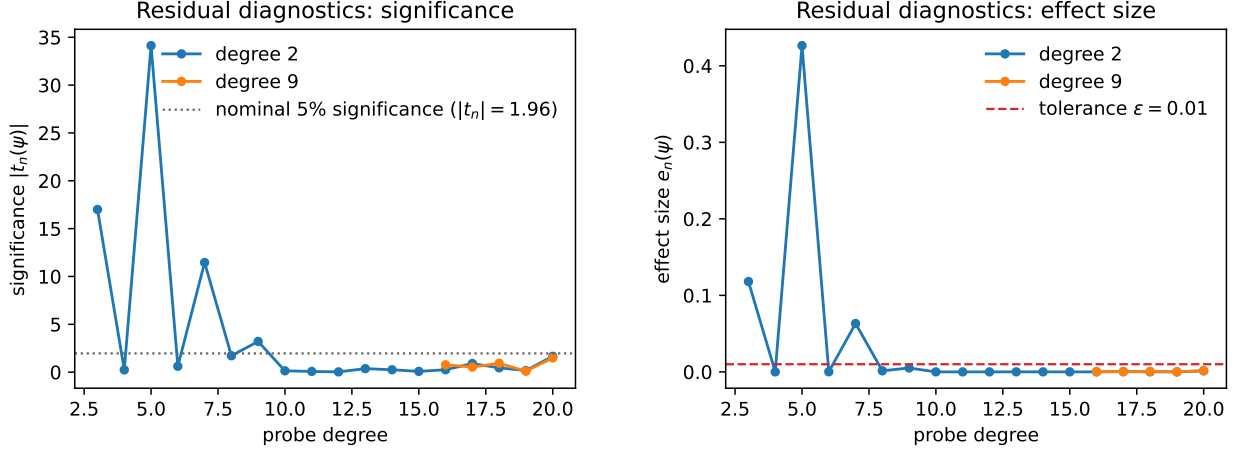


Figure 3. Residual–feature diagnostics for the two-branch example, for the degree-2 (underfit) and degree-9 (high-capacity) least-squares fits, evaluated on out-of-basis Legendre probes. Top: significance  $|t_n(P_k)|$ , with the nominal 5% line  $|t_n| = 1.96$ . Bottom: effect size  $e_n(P_k)$ , the fraction of residual variance a correction along  $P_k$  would remove, with the task tolerance  $\varepsilon = 0.01$ . The degree-2 residual is both significant and large (Regime I); the degree-9 residual is neither (Regime III) and its mean-square equals the aleatoric floor.

## 6.2. A closure-modeling example: two-scale Lorenz–96

We now turn to a setting closer to computational science and engineering, where the population quantities are not available in closed form. The purpose is not to benchmark closure models, but to show how the diagnostic framework can be used when the conditional-mean barrier must be inferred from data.

We use the two-scale Lorenz–96 system [46, 47]

$$\dot{X}_k = (X_{k+1} - X_{k-2})X_{k-1} - X_k + F - \frac{hc}{b} \sum_{j=1}^J Y_{j,k}, \quad (24)$$

$$\dot{Y}_{j,k} = -cbY_{j+1,k}(Y_{j+2,k} - Y_{j-1,k}) - cY_{j,k} + \frac{hc}{b} X_k, \quad (25)$$

with periodic indexing in both  $k$  and  $j$ . The slow variables  $\{X_k\}_{k=1}^K$  are resolved, while the fast variables  $\{Y_{j,k}\}$  are treated as unresolved. The unresolved forcing acting on the  $k$ -th slow variable is

$$C_{t,k} = -\frac{hc}{b} \sum_{j=1}^J Y_{j,k}(t). \quad (26)$$

The closure problem is to approximate  $C_{t,k}$  from resolved information. In this experiment we choose the local stencil

$$S_{t,k} = (X_{k-1}(t), X_k(t), X_{k+1}(t)) \quad (27)$$

as the descriptor and fit deterministic maps

$$\hat{f}_p(S_{t,k}) \approx C_{t,k}.$$

This choice is intentionally local and interpretable. A wider stencil or time delay embeddings would define a different conditioning variable and hence a different conditional law; here we ask what can be learned from the fixed local stencil (27).

We use  $K = J = 8$ ,  $F = 10$ ,  $h = 2$ , and  $c = b = 10$ . The full two-scale system is integrated with time step  $\Delta t = 5 \times 10^{-3}$ . After a burn-in period, the trajectory is downsampled to reduce short-time correlation and then split into time blocks. The retained data contain 300 snapshots, hence  $300K = 2400$  local stencil–closure pairs. The first 180 snapshots are used for fitting, the next 60 for diagnostics, and the last 60 for held-out one-step evaluation.

For each degree  $p$ , we fit a total-degree polynomial closure  $\hat{f}_p$  on standardized stencil variables by least squares. Figure 4(a) shows the one-step closure accuracy: the train, diagnostic, and test  $R^2$  all rise rapidly from  $p = 1$  to  $p = 3$  and then saturate, with the test  $R^2$  remaining slightly below the diagnostic  $R^2$  throughout.

We select the representative closure by Procedure 1. The probe family is the monomials of the standardized stencil up to total degree 6; a probe is *out-of-basis* for a degree- $p$  fit if its total degree exceeds  $p$ . For each fit we compute the effect size  $e_n(\psi)$  of (6) on the diagnostic snapshots—the fraction of residual variance a correction along  $\psi$  would remove. Because  $e_n$  is a ratio of second moments, it is unaffected by the spatial correlation among the  $K$  stencils recorded at one time step, so it can be read directly. Figure 4(b) plots  $\max_{\psi} e_n(\psi)$  over the out-of-basis probes against the fitted degree, with the task tolerance fixed at  $\varepsilon = 0.01$ , the same value as in Section 6.1. The maximum falls

$$\max_{\psi} e_n : 0.193 \longrightarrow 0.047 \longrightarrow 0.0034$$

from  $p = 1$  to  $p = 3$ , crossing  $\varepsilon$  at  $p = 3$  and remaining below it for  $p = 4, 5$ : enriching the basis further removes no practically large structure, so the stop rule is satisfied at  $p = 3$ . We adopt this degree, which also keeps the model simple and stable for closed-loop simulation. For the selected model,

$$R_{\text{diag}}^2 = 0.743, \quad R_{\text{test}}^2 = 0.684.$$

Equivalently, the residual mean-square on the diagnostic set is  $\hat{\sigma}_r^2 \approx 1.82$  against a forcing variance of 7.10, so that about 26% of the unresolved forcing is irreducible from this stencil. Once the stop rule holds, this  $\hat{\sigma}_r^2$  is the empirical estimate of the aleatoric floor  $\mathbb{E}[\text{Var}(C | S)]$ , which is not available in closed form here (Section 3.3). The  $p = 3$  closure therefore sits at the conditional-mean barrier (Regime III of Table 1).

A significance test corroborates the selection. Because the  $K = 8$  stencils in a snapshot are spatially correlated, raw per-row significance would be overstated; we therefore form a snapshot-clustered statistic, averaging the row product  $r_{t,k}\psi(S_{t,k})$  within each snapshot to a snapshot moment  $H_t = K^{-1} \sum_k r_{t,k}\psi(S_{t,k})$  and computing the one-sample  $t$ -statistic  $t_{59}(\psi) = \sqrt{60} \bar{H} / \hat{s}_H$ . The clustered  $\max_{\psi} |t_{59}|$  over out-of-basis probes falls  $7.96 \rightarrow 4.84 \rightarrow 1.43$  across  $p = 1, 2, 3$ , dropping below the Bonferroni-corrected 5% threshold ( $|t| \approx 3.6$ ) at  $p = 3$ , in agreement with the effect size. Consistent with the supporting role significance plays in Section 3.3, we treat the effect size as the primary criterion and the clustered test as a check.

Reaching the barrier does not mean the forcing is determined by the local stencil: a large conditional spread can persist around the learned mean. To visualize this, Figure 4(c) partitions the diagnostic pairs  $(S_{t,k}, C_{t,k})$  into ten bins by the value of the central stencil component  $X_k$ , and plots the standard deviation of the true forcing  $\text{std}(C | X_k)$  and of the post-closure residual  $\text{std}(C - \hat{f}_3 | X_k)$  against the bin mean of  $X_k$ . Across the range of the resolved state the two curves nearly coincide, so the deterministic closure removes little of the spread.

Finally, we examine what happens when the fitted deterministic closure is embedded into an autonomous slow-only model,

$$\tilde{X}_k = (\tilde{X}_{k+1} - \tilde{X}_{k-2})\tilde{X}_{k-1} - \tilde{X}_k + F + \hat{f}_3(\tilde{S}_k), \quad (28)$$

where

$$\tilde{S}_k = (\tilde{X}_{k-1}, \tilde{X}_k, \tilde{X}_{k+1}).$$

The rollout comparison is deliberately separate from the previously used dataset. We generate new long trajectories of both the full two-scale reference system and the closed slow-only system starting from the same initial condition, discard burn-in, and compare downstream statistics.

The one-point marginal variance of  $X_k$  is nearly preserved:

$$\frac{\text{Var}_{\text{closed}}(X_k)}{\text{Var}_{\text{ref}}(X_k)} \approx 1.000.$$

This is an important caution: the closed slow-only system is itself a nonlinear dynamical system with its own attractor, so its one-point marginals can match those of the reference even when its joint or time-aggregated statistics do not. The more revealing statistic is the slow energy

$$E(t) = \frac{1}{2K} \sum_{k=1}^K X_k(t)^2. \quad (29)$$

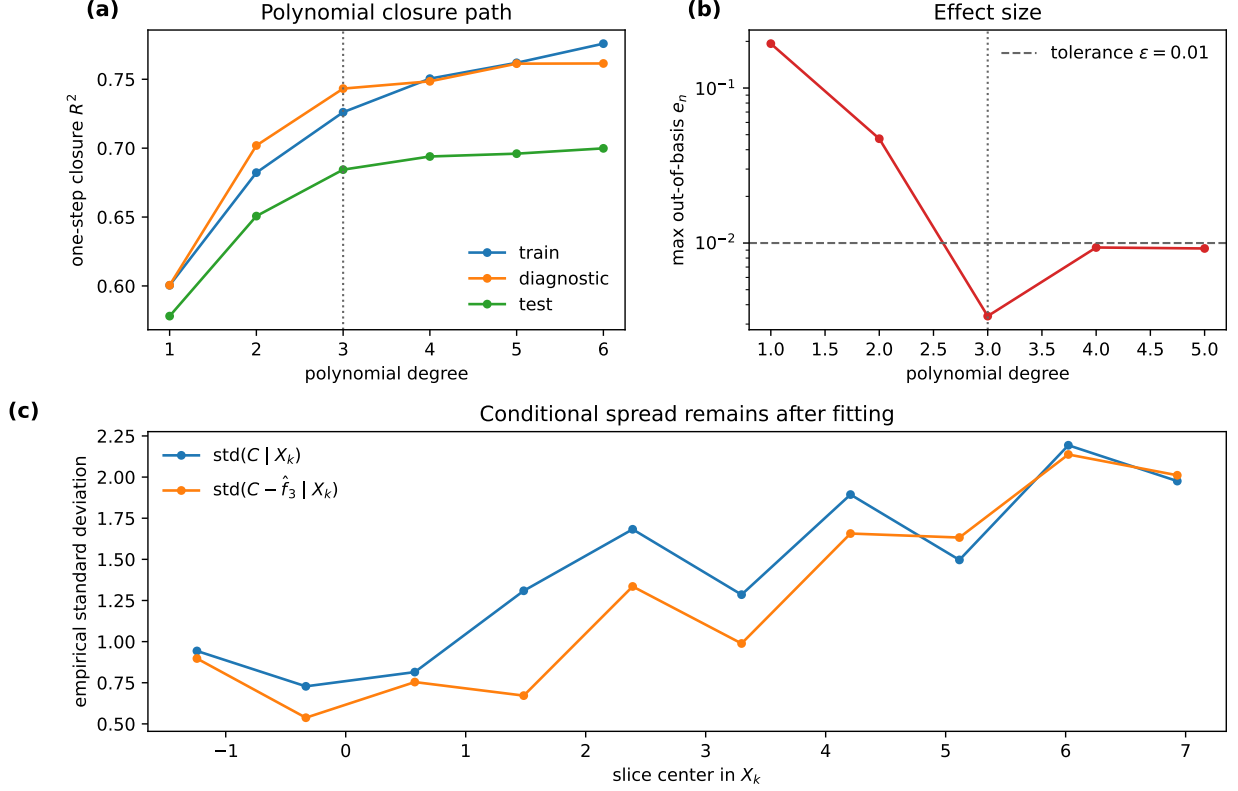


Figure 4. Diagnostic results for the two-scale Lorenz-96 closure. (a) One-step closure  $R^2$  (train, diagnostic, test) versus polynomial degree, saturating by  $p = 3$  (dotted line: selected closure). (b) Primary diagnostic: the maximum out-of-basis effect size  $\max_{\psi} e_n(\psi)$  versus degree (log scale), with the task tolerance  $\epsilon = 0.01$ ; the maximum drops below  $\epsilon$  at  $p = 3$ , locating the conditional-mean barrier. (c) Conditional spread after mean fitting: within ten bins of the central stencil component  $X_k$  (neighbors  $X_{k\pm 1}$  free), the standard deviation of the true forcing  $\text{std}(C | X_k)$  and of the post-closure residual  $\text{std}(C - \hat{f}_3 | X_k)$ .

For this quantity the deterministic closure strongly suppresses fluctuations. Table 3 summarizes the contrast, and the slow-energy densities of Figure 5(a) show the prediction much narrower than the reference, its variance reduced to 4.6% of the reference value, although the marginal variance of  $X_k$  is essentially unchanged.

The slow-energy trajectory of Figure 5(b) shows the dynamical side of the same effect: the closed deterministic system fluctuates in a visibly smaller band, while the space-time windows of Figure A.6 confirm that the closed system remains dynamically active. The issue is not collapse to a constant state but distortion of collective fluctuations. This illustrates the practical form of the conditional-mean barrier in closure modeling: fitting the mean is not the same as modeling the conditional law.

### 6.3. Adding a learned stochastic scale

Section 6.2 established that the degree-3 deterministic closure sits at the conditional-mean barrier (Regime III): it has reached the conditional mean on the local stencil, yet a large irreducible spread remains, and that spread is what the autonomous rollout suppresses. By Proposition 4.1 this barrier cannot be crossed within squared loss; it requires a loss that scores distributions (Section 5). We now make the minimal such change—keeping the deterministic mean closure fixed and learning only a conditional scale around it by negative log-likelihood.

Let  $\hat{f}_3(S)$  denote the selected deterministic least-squares closure from Section 6.2. We fit a heteroscedastic Gaussian approximation

$$C_{t,k} | S_{t,k} \approx \mathcal{N}(\hat{f}_3(S_{t,k}), \hat{\sigma}(S_{t,k})^2),$$

Statistic	Closed/reference ratio	Interpretation
$\text{Var}(X_k)$	1.000	one-point marginal variance preserved
$\text{Var}(E)$	0.046	collective energy fluctuations suppressed

Table 3. Downstream statistics from independent long rollouts of the full two-scale reference system and the closed deterministic slow-only system.

where  $\hat{f}_3$  is frozen and only  $\hat{\sigma}$  is trained. Equivalently, on the fixed residuals

$$r_{t,k} = C_{t,k} - \hat{f}_3(S_{t,k}),$$

we minimize the Gaussian negative log-likelihood

$$\mathcal{L}_{\text{scale}} = \frac{1}{n} \sum_i \left[ \log \sigma_\theta(S_i) + \frac{r_i^2}{2\sigma_\theta(S_i)^2} \right], \quad (30)$$

up to the irrelevant constant  $\frac{1}{2} \log(2\pi)$ . The log-scale is modeled by a low-degree polynomial and lightly regularized. Freezing the mean is important: jointly fitting a heteroscedastic likelihood also reweights the mean, which can change the closed-loop drift even when one-step scores remain reasonable. On the diagnostic split, the standardized residual  $(C - \hat{f}_3(S))/\hat{\sigma}(S)$  has empirical standard deviation 0.994, with 71.3% and 94.4% of samples within one and two standard deviations, respectively.

To test the dynamical effect of this learned scale, we use a time-discrete random-force closure

$$C_k^n = \hat{f}_3(S_k^n) + \hat{\sigma}(S_k^n) \xi_k^n, \quad \xi_k^n \sim \mathcal{N}(0, 1), \quad (31)$$

inside the slow-only Lorenz–96 model. This is not interpreted as an Euler–Maruyama discretization of a continuous-time diffusion; it is an illustrative way to inject the learned conditional spread of the instantaneous closure forcing. During rollout, extreme polynomial extrapolations of the log-scale are capped as a numerical safeguard.

Figure 5 compares the full two-scale reference system, the deterministic slow-only model using  $\hat{f}_3$ , and the stochastic slow-only model using (31). Panel (a) shows the slow-energy density for all three systems: the deterministic mean closure produces a much narrower energy distribution, while the stochastic closure broadens it toward the reference. Panel (b) shows representative slow-energy trajectories, making the same contrast visible in time. Space–time windows of all three rollouts, confirming that the closed systems remain dynamically active, are collected in Figure A.6.

Both closed models preserve the one-point variance of  $X_k$  and the mean slow energy reasonably well, but they differ strongly in the collective fluctuation statistic:

$$\frac{\text{Var}_{\text{det}}(E)}{\text{Var}_{\text{ref}}(E)} \approx 0.046, \quad \frac{\text{Var}_{\text{stoch}}(E)}{\text{Var}_{\text{ref}}(E)} \approx 0.531.$$

Thus the stochastic closure does not exactly reproduce the reference energy statistics. The Gaussian scale model captures only a low-order approximation of the conditional residual law, and the random-force rollout uses a simple time-discrete coupling rather than a learned temporal process. These choices already substantially reduce the energy-variance suppression of the deterministic mean closure, but they do not fully recover the reference statistics. More expressive conditional generators and richer conditioning variables may further improve the recovery.

## 7. Conclusions

This tutorial has developed the conditional-mean barrier as a practical way to understand when deterministic squared-loss regression reaches its natural limit. The key point is: under squared loss, a sufficiently expressive predictor targets the conditional mean, not the full conditional law. Residual–feature orthogonality and the explained-variance ceiling provide diagnostics for recognizing this situation in data, while the variance-suppression theorem shows why adding latent randomness to a squared-loss-trained predictor does not overcome the barrier.

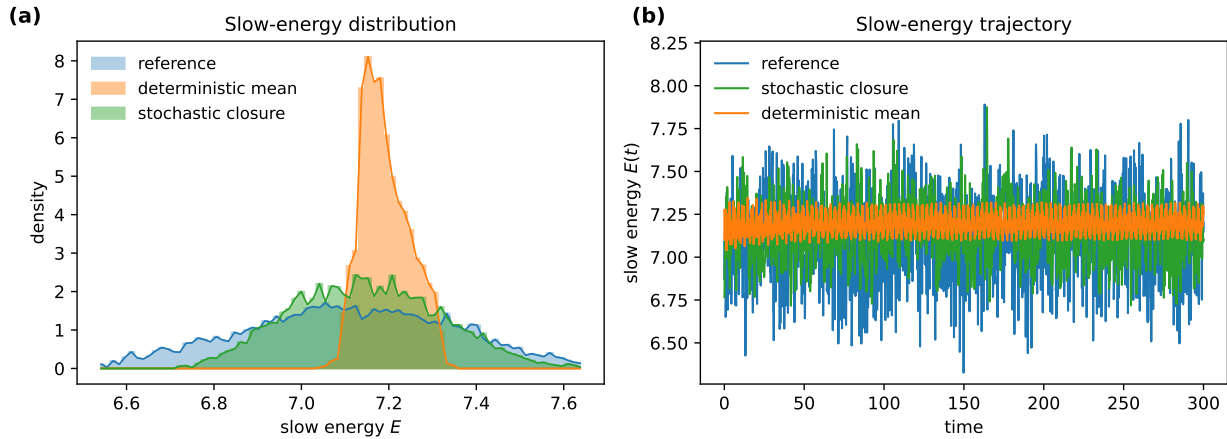


Figure 5. Lorenz-96 slow-energy statistics from independent long rollouts of the reference, deterministic-mean, and stochastic closures. (a) Slow-energy densities. (b) Slow-energy trajectories.

For students and practitioners, the conditional-mean barrier offers a compact decision procedure built on two questions. First, does the residual still carry reducible structure? Second, granting that no more structure can be extracted, is the remaining variance small enough for the task? If reducible structure remains and matters, one improves the deterministic model; if the predictor has reached the conditional mean but the residual variability matters, the question has changed, and one must move from fitting a function to learning some feature of  $P(Y | X)$ . The loss function is therefore not a technical afterthought; it determines what object is learned.

## Appendix A. Space–time rollouts for the Lorenz-96 closures

Here we display the space–time windows of the resolved variables  $X_k$  for the three Lorenz-96 systems discussed in the main article: the full two-scale reference system, the deterministic-mean closed slow-only system, and the stochastic closed slow-only system. These windows accompany the downstream slow-energy statistics reported in the main text; their role is to confirm that each closed system remains dynamically active rather than collapsing to a fixed state.

## References

- [1] S. L. Brunton, J. L. Proctor, J. N. Kutz, Discovering governing equations from data by sparse identification of nonlinear dynamical systems, *Proceedings of the National Academy of Sciences* 113 (15) (2016) 3932–3937.
- [2] S. H. Rudy, S. L. Brunton, J. L. Proctor, J. N. Kutz, Data-driven discovery of partial differential equations, *Science Advances* 3 (4) (2017) e1602614.
- [3] K. Duraisamy, G. Iaccarino, H. Xiao, Turbulence modeling in the age of data, *Annual Review of Fluid Mechanics* 51 (1) (2019) 357–377.
- [4] L. Lu, P. Jin, G. Pang, Z. Zhang, G. E. Karniadakis, Learning nonlinear operators via DeepONet based on the universal approximation theorem of operators, *Nature Machine Intelligence* 3 (3) (2021) 218–229.
- [5] N. Kovachki, Z. Li, B. Liu, K. Azizzadenesheli, K. Bhattacharya, A. Stuart, A. Anandkumar, Neural operator: Learning maps between function spaces with applications to PDEs, *Journal of Machine Learning Research* 24 (89) (2023) 1–97.
- [6] P. C. Hansen, *Discrete inverse problems: Insight and algorithms*, Society for Industrial and Applied Mathematics, 2010.
- [7] M. Benning, M. Burger, Modern regularization methods for inverse problems, *Acta Numerica* 27 (2018) 1–111.
- [8] A. J. Chorin, O. H. Hald, R. Kupferman, Optimal prediction and the Mori–Zwanzig representation of irreversible processes, *Proceedings of the National Academy of Sciences* 97 (7) (2000) 2968–2973.
- [9] F. Lu, K. K. Lin, A. J. Chorin, Data-based stochastic model reduction for the Kuramoto–Sivashinsky equation, *Physica D* 340 (2017) 46–57.
- [10] C. J. Gommers, Y. Jiao, S. Torquato, Microstructural degeneracy associated with a two-point correlation function and its information content, *Physical Review E* 85 (5) (2012) 051140.
- [11] R. Bostanabad, Y. Zhang, X. Li, et al., Computational microstructure characterization and reconstruction: Review of the state-of-the-art techniques, *Progress in Materials Science* 95 (2018) 1–41.
- [12] C. Ledig, L. Theis, F. Huszár, J. Caballero, A. Cunningham, A. Acosta, A. Aitken, A. Tejani, J. Totz, Z. Wang, W. Shi, Photo-realistic single image super-resolution using a generative adversarial network, in: *Proceedings of the IEEE Conference on Computer Vision and Pattern Recognition*, 2017, pp. 4681–4690.

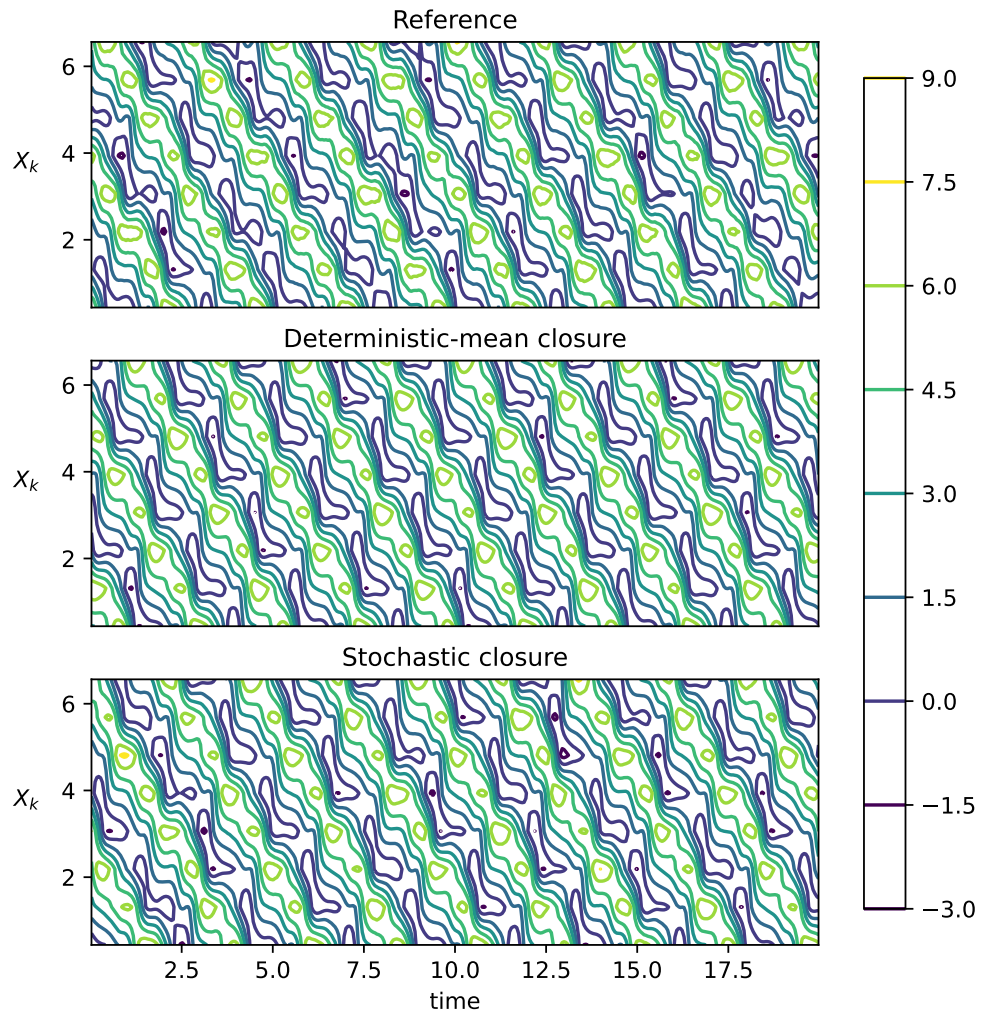


Figure A.6. Short space–time windows of the resolved variables  $X_k$  from independent long rollouts, on a shared color scale: the full two-scale reference system (top), the deterministic-mean closed slow-only system (middle), and the stochastic closed slow-only system (bottom). All three remain dynamically active rather than collapsing to a fixed state.

- [13] C. Saharia, J. Ho, W. Chan, T. Salimans, D. J. Fleet, M. Norouzi, Image super-resolution via iterative refinement, *IEEE Transactions on Pattern Analysis and Machine Intelligence* 45 (4) (2023) 4713–4726.
- [14] T. Hastie, R. Tibshirani, J. Friedman, *The Elements of Statistical Learning: Data Mining, Inference, and Prediction*, 2nd Edition, Springer, New York, 2009.
- [15] C. M. Bishop, *Pattern recognition and machine learning*, Springer, 2006.
- [16] T. M. Cover, J. A. Thomas, *Elements of information theory*, 2nd Edition, John Wiley & Sons, Hoboken, NJ, 2006.
- [17] I. Goodfellow, J. Pouget-Abadie, M. Mirza, B. Xu, D. Warde-Farley, S. Ozair, A. Courville, Y. Bengio, Generative adversarial nets, in: *Advances in Neural Information Processing Systems*, Vol. 27, 2014, pp. 2672–2680.
- [18] Y. Song, J. Sohl-Dickstein, D. P. Kingma, A. Kumar, S. Ermon, B. Poole, Score-based generative modeling through stochastic differential equations, in: *International Conference on Learning Representations*, 2021.
- [19] O. Kallenberg, *Foundations of Modern Probability*, 2nd Edition, Springer, New York, 2002.
- [20] M. Mohri, A. Rostamizadeh, A. Talwalkar, *Foundations of machine learning*, MIT press, 2018.
- [21] I. Steinwart, On the influence of the kernel on the consistency of support vector machines, *Journal of Machine Learning Research* 2 (Nov) (2001) 67–93.
- [22] R. Schaback, H. Wendland, Kernel techniques: from machine learning to meshless methods, *Acta Numerica* 15 (2006) 543–639.
- [23] K. Hornik, Approximation capabilities of multilayer feedforward networks, *Neural Networks* 4 (1991) 251–257.
- [24] C. F. Higham, D. J. Higham, Deep learning: An introduction for applied mathematicians, *SIAM Review* 61 (4) (2019) 860–891.
- [25] G. Cybenko, Approximation by superpositions of a sigmoidal function, *Mathematics of Control, Signals and Systems* 2 (1989) 303–314.
- [26] M. Leshno, V. Y. Lin, A. Pinkus, S. Schocken, Multilayer feedforward networks with a nonpolynomial activation function can approximate any function, *Neural Networks* 6 (1993) 861–867.
- [27] L. P. Hansen, Large sample properties of generalized method of moments estimators, *Econometrica* 50 (1982) 1029–1054.
- [28] L. Wasserman, *All of Statistics: A Concise Course in Statistical Inference*, Springer, New York, 2004.
- [29] D. A. Nix, A. S. Weigend, Estimating the mean and variance of the target probability distribution, in: *Proceedings of the IEEE International Conference on Neural Networks*, 1994, pp. 55–60.
- [30] E. M. Stein, R. Shakarchi, *Measure theory, integration, and Hilbert spaces* (2005).
- [31] D. P. Kingma, M. Welling, Auto-encoding variational Bayes, in: *International Conference on Learning Representations*, 2014.
- [32] A. Kendall, Y. Gal, What uncertainties do we need in Bayesian deep learning for computer vision?, in: *Advances in Neural Information Processing Systems*, Vol. 30, 2017, pp. 5574–5584.
- [33] A. P. Guillaumin, L. Zanna, Stochastic-deep learning parameterization of ocean momentum forcing, *Journal of Advances in Modeling Earth Systems* 13 (9) (2021) e2021MS002534.
- [34] G. Papamakarios, E. Nalisnick, D. J. Rezende, S. Mohamed, B. Lakshminarayanan, Normalizing flows for probabilistic modeling and inference, *Journal of Machine Learning Research* 22 (57) (2021) 1–64.
- [35] L. Guo, H. Wu, T. Zhou, Normalizing field flows: Solving forward and inverse stochastic differential equations using physics-informed flow models, *Journal of Computational Physics* 461 (2022) 111202.
- [36] M. Yang, P. Wang, D. del Castillo-Negrete, Y. Cao, G. Zhang, A pseudoreversible normalizing flow for stochastic dynamical systems with various initial distributions, *SIAM Journal on Scientific Computing* 46 (4) (2024) C508–C533.
- [37] E. Cleary, A. Garbuno-Inigo, S. Lan, T. Schneider, A. M. Stuart, Calibrate, emulate, sample, *Journal of Computational Physics* 424 (2021) 109716.
- [38] D. Qi, J. Harlim, A data-driven statistical-stochastic surrogate modeling strategy for complex nonlinear non-stationary dynamics, *Journal of Computational Physics* 485 (2023) 112085.
- [39] D. J. Rezende, S. Mohamed, D. Wierstra, Stochastic backpropagation and approximate inference in deep generative models, in: *Proceedings of the 31st International Conference on Machine Learning*, 2014, pp. 1278–1286.
- [40] K. Gundersen, A. Oleynik, N. Blaser, G. Alendal, Semi-conditional variational auto-encoder for flow reconstruction and uncertainty quantification from limited observations, *Physics of Fluids* 33 (1).
- [41] M. Mirza, S. Osindero, Conditional generative adversarial nets (2014). [arXiv: 1411.1784](https://arxiv.org/abs/1411.1784).
- [42] L. Yang, D. Zhang, G. E. Karniadakis, Physics-informed generative adversarial networks for stochastic differential equations, *SIAM Journal on Scientific Computing* 42 (1) (2020) A292–A317.
- [43] J. Ho, A. Jain, P. Abbeel, Denoising diffusion probabilistic models, in: *Advances in Neural Information Processing Systems*, Vol. 33, 2020, pp. 6840–6851.
- [44] P. Vincent, A connection between score matching and denoising autoencoders, *Neural Computation* 23 (2011) 1661–1674.
- [45] Y. Liu, Y. Chen, D. Xiu, G. Zhang, A training-free conditional diffusion model for learning stochastic dynamical systems, *SIAM Journal on Scientific Computing* 47 (5) (2025) C1144–C1171.
- [46] E. N. Lorenz, Predictability: A problem partly solved, in: *Proc. Seminar on Predictability*, Vol. 1, Reading, 1996, pp. 1–18.
- [47] D. S. Wilks, Effects of stochastic parametrizations in the Lorenz’96 system, *Quarterly Journal of the Royal Meteorological Society* 131 (606) (2005) 389–407.